Diffuse Reflectance Spectroscopy Can Differentiate High Grade and Low Grade Prostatic Carcinoma

Priya N. Werahera*, Senior Member IEEE, Edward A. Jasion, E. David Crawford, M. Scott Lucia, Adrie van Bokhoven, Holly T. Sullivan, Fernando J. Kim, Paul D. Maroni, J. David Port, John W. Daily, and Francisco G. La Rosa

***Abstract*— Prostate tumors are graded by the *revised* Gleason Score (GS) which is the sum of the two predominant Gleason grades present ranging from 6-10. GS 6 cancer exclusively with Gleason grade 3 is designated as low grade (LG) and correlates with better clinical prognosis for patients. GS ≥7 cancer with at least one of the Gleason grades 4 and 5 is designated as HG indicate worse prognosis for patients. Current transrectal ultrasound guided prostate biopsies often fail to correctly diagnose HG prostate cancer due to sampling errors. Diffuse reflectance spectra (DRS) of biological tissue depend on tissue morphology and architecture. Thus, DRS could potentially differentiate between HG and LG prostatic carcinoma. A 15-gauge optical biopsy needle was prototyped to take prostate biopsies after measuring DRS with a laboratory fluorometer. This needle has an optical sensor that utilizes 8x100 µm optical fibers for tissue excitation and a single 200 µm central optical fiber to measure DRS. Tissue biopsy cores were obtained from 20 surgically excised prostates using this needle after measuring DRS at 5 nm intervals between 500-700 nm wavelengths. Tissue within a measurement window was histopathologically classified as either benign, LG, or HG and correlated with DRS. Partial least square analysis of DRS identified principal components (PC) as potential classifiers. Statistically significant PCs ($p<0.05$) were tested for their ability to classify biopsy tissue using support vector machine and leave-one-out cross validation method. There were 29 HG and 49 LG cancers among 187 biopsy cores included in the study. Study results show 76% sensitivity, 80% specificity, 93% negative predictive value, and 50% positive predictive value for HG versus benign, and 76%, 73%, 84%, and 63%, for HG versus LG prostate tissue classification. DRS failed to diagnose 7/29 (24%) HG cancers. This study demonstrated that an optical biopsy needle guided by DRS has sufficient accuracy to differentiate HG from LG carcinoma and benign tissue. It may allow precise targeting of HG prostate cancer providing more accurate assessment of the disease and improvement in patient care.**

Research supported by a proof-of-concept grant from the Precision Biopsy, Inc., a subsidiary of Allied Minds, Inc., Boston, MA.

P. N. Werahera is with the Pathology and Bioengineering Departments, University of Colorado Anschutz Medical Campus, Mail Stop 8104, P. O. Box 6511, Aurora, CO 80045. (phone: 303-724-3784; fax: 303-724-3712; e-mail: Priya.Werahera@ucdenver.edu)

E. A. Jasion is with the Precision Biopsy Inc., 12705 E. Montview Blvd #350, Aurora, CO 80045.

F. G. La Rosa, M. S. Lucia, A. van Bokhoven, and H. T. Sullivan are with the Pathology Department, P. D. Maroni and F. J. Kim are with the Department of Surgery, J. D. Port is with Pharmacology Department, and E. D. Crawford is with the Urologic Oncology Department, University of Colorado Anschutz Medical Campus, Aurora, CO 80045.

J. W. Daily is with the Mechanical Engineering Department, University of Colorado, Boulder, CO 80309.

P. N. Werahera, M. S. Lucia, and J. W. Daily are the co-founders of Precision Biopsy Inc., 12705 E. Montview Blvd #350, Aurora, CO 80045.

I. Introduction

Prostate cancer remains a major health concern for men of North America and Europe. In 2016, it is estimated that 180,890 men will be diagnosed with prostate cancer and 26,120 men will die from this disease in the United States alone [1]. Disease is diagnosed by pathological examination of biopsy tissue obtained from patients suspected of having the disease [2]. Urologists take 10-12 transrectal ultrasound (TRUS) guided biopsies per patient using an 18-gauge (1.27 mm) biopsy needle and pathologists diagnose and grade prostate tumors using the Gleason scoring system [3].

The Gleason scoring system has been revised recently [4]. Only three Gleason grades 3-5 are currently recognized in the revised system instead of the five original Gleason grades 1-5 as shown in *Fig. 1*. Original Gleason grades 1 & 2 are now included within the Gleason grade 3 tumors and considered to be non-aggressive [5]. Gleason grades 4 & 5 tumors are considered more aggressive with metastatic potential and worse clinical outcomes [6].

Gleason grades depend on the architectural pattern of the malignant glands. Gleason grade 3 is characterized by independent unfused malignant glands. Fusion of two or more glands, and cribriform or glomerular patterns, are distinctive of Gleason grade 4. In Gleason grade 5, the glandular configuration is lost and the tumor cells are arranged in sheets and single cells.

Prostate tumors are heterogeneous in terms of grade and behave according to the composition of grades within the tumor. Thus, tumors are graded by the sum of the two most important grades present as a Gleason Score (GS) ranging from 6 to 10. Tumors of GS 6 (3+3) are considered low grade (LG) while GS ≥7 with Gleason grades 4 & 5 are high

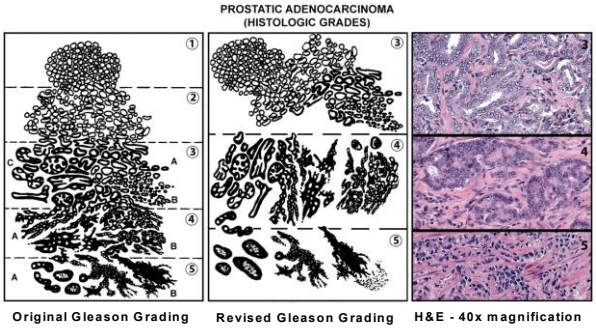

Figure 1: Original (left) and revised (center) patterns of Gleason grading, as compared with corresponding H&E stained images of revised Gleason patterns 3, 4, and 5 (right).

grade (HG). GS is currently the *best* prognostic variable available to predict the clinical outcome of this disease.

At present, 60-65% of patients diagnosed by TRUS guided prostate biopsies have GS 6 cancer [6]. However, TRUS biopsies may over- or underestimate GS due to sampling errors and interobserver variabilities. Two studies found 25-42% of patients with GS 6 were upgraded to GS ≥7 while 14% of patients with GS ≥7 were downgraded to GS 6 following prostatectomy surgery [7;8]. When left undiagnosed, HG cancers are at high risk of spreading beyond the prostate gland and metastasizing to distant sites with the consequent increased mortality. Hence, assessing *correct GS* at the time of biopsy is crucial in deciding the best treatment option for each patient [7].

Diagnostic accuracy of TRUS biopsies can be improved by classifying underlying tissue using optical spectroscopy as a precursor to biopsy. There are several advantages of using optical spectroscopy for cancer diagnosis; it is quantitative, fast, and sensitivity to intrinsic biomarkers of tissue such as histopathological grade. In diffuse reflectance spectroscopy, light is delivered to tissue and after several successive scattering and absorption events it re-emerges from the tissue bearing information regarding size and shape of cells and intracellular structures of tissue underneath [9]. The Gleason scoring system relies on the architecture of the malignant glands and cells [3]. Thus, diffuse reflectance spectra (DRS) could potentially diagnose prostate cancer as well as classify histopathological grade of the disease.

A'Amar et al. used DRS for *ex vivo* prostate tissue classification [10]. DRS within 330-760 nm were collected using a fiber optic probe consists of two fibers, 1x400 µm fiber for illumination and 1x200 µm fiber for collection. They reported 83% sensitivity, 87% specificity, and 95% negative predictive value for distinguishing dysplastic prostatic tissue from benign prostatic tissue. Dysplastic prostate tissue included low and high grade prostatic intra-epithelial neoplasia (PIN and HG-PIN), and prostatic adenocarcinoma.

Sharma et al. used DRS and auto-fluorescence lifetime spectroscopy (AFLS) for classification of prostate tissue from fresh surgically excised prostates [11]. DRS were measured between 500-840 nm. AFLS used excitation at 447 nm and measured lifetime at four emission wavelengths of 532, 562, 632, and 684 nm. Spectra were collected using a custom-made fiber optic probe with 1 mm outer diameter containing four fibers of diameters 2x200, 1x100, and 1x400 µm. They showed 63.0±1.5% sensitivity and 82.9±1.6% specificity for GS ≥7 versus benign tissue classification using *only* DRS; 64.2±2.5% and 69.2±1.8%, respectively, using *only* AFLS; 79.0±1.7% and 85.2±1.1%, respectively, using combined DRS and AFLS. The main limitation was the lack of GS 6 cancer as nearly two thirds of patients diagnosed by prostate biopsies have GS 6 cancer [6].

We have prototyped an optical biopsy needle to obtain prostate biopsies *after* optical characterization of underlying tissue to be sampled [12]. In this paper, we present analyses of the DRS and biopsy data obtained from this needle for the purpose of prostate tissue classification correlated to histopathological grade. In Section II we present the experimental setup for the optical biopsy needle and spectral data analyses for prostate tissue classification. Experimental results for tissue classification are provided in Section III and conclusions are given in Section IV.

II. METHODOLOGY

A. Experimental Setup

Fig.2 shows the experimental setup used to collect DRS from *ex vivo* prostates. It includes the optical biopsy needle, fluorometer with fiber-optic platform, and fresh surgically excised prostatectomy specimens. The optical biopsy needle consists of a 15-gauge (1.79 mm) outer needle, slightly smaller inner needle, and two optical connectors. The working length of the needle is 18 cm. The inner needle has an optical sensor at the tip with a 22 mm long specimen notch. The fiber optic cables are placed underneath the specimen notch. Outer and inner needles are designed to interface with the BARD Urological MAGNUM® gun.

The tip of the inner needle has to be cut and polished at an angle to facilitate tissue cutting. However, the critical angle must be determined in order to minimize reflective losses for light travelling from the optical sensor into the tissue. This critical angle was ~60 degree according to the Snell's law of refraction calculated using refractive indices of 1.491at 290 nm and 1.478 at 340 nm for glass fiber and 1.385 for mammalian HeLa cells.

The front-ends of the fibers are terminated at the tip of the inner needle and arranged as the optical sensor in 8 around 1 configuration. The back-ends of the fibers are terminated with two standard SMA connectors and serve as an interface to a standard laboratory fluorometer (Fluorolog-3, JY HORIBA) through an optical platform (F-3000) as shown in *Fig 2*. The Fluorolog-3 consists of a 450W xenon arc lamp as the excitation source, a monochromator as the excitation wavelength selector, a 2nd monochromator to select the emission spectra from the sample, and an R928P photon multiplier tube in photon-counting mode as the emission detector. DRS of prostate tissue were collected between 500 to 700 nm at 5 nm intervals while operating the Fluorolog-3 in synchronous scan mode. Background measurements were taken by inserting the biopsy needle in a test tube with deionized water.

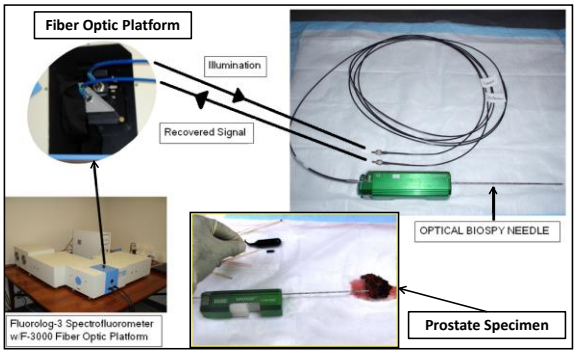

Figure 2: Experimental setup for measuring DRS of prostate tissue using 15G optical biopsy needle and Fluorolog-3

The experimental procedures involving human subjects described in this paper were approved by the Colorado Multiple Institutional Review Board. Consented study patients were scheduled to have radical prostatectomy surgery at the University of Colorado Hospital between April 2009 and June 2010. Surgically excised prostates were delivered to the lab within minutes. Optical data and corresponding tissue biopsy cores were taken within a 90 min period from surgical excision. Prostates were placed in a specimen container with 10% neutral buffered formalin (NBF) after data collection. Spectral data and corresponding tissue biopsy cores were obtained from 10-12 random locations within each prostate specimen. The distal-end of each biopsy core was inked and put inside a specimen vial containing 10% NBF. Each specimen vial was labeled accordingly for correlation with spectral data.

B. Data Analysis

Standard H&E slides were prepared from formalin-fixed biopsy cores for histopathological examination. The exact location of the tissue core where optical data collected was calculated based on the geometries of the needle and BARD Magnum gun. This *measurement window* was 0.5 mm wide and located 1.7 mm from the distal-end of the core as shown in *Fig. 3*. Some biopsy cores were not included in the study due to either fragmentation errors (cores were broken) or off-setting errors (cores were not correctly placed at the distal-end of the needle). Histopathology of these cores could not be reliably correlated with spectral data.

The tissue within the *measurement window* was classified as either benign or cancer. Benign category included biopsies that did not show any evidence of malignancy within the *measurement window*. Cancer tissue was indicated with a GS and the percentage of involvement in that window, extending from 5% to 100% at 5% increments. For example, *Fig. 3* shows GS 7 (3+4) cancer with 80% involvement that indicates 80% of tissue within the *measurement window* is cancer of GS 7 and 20% is benign tissue. Benign tissue may include stroma, glandular atrophy, benign prostatic hyperplasia (BPH), prostatitis, *etc*.

Biopsy cores were divided into three diagnostic categories based on histopathology examination: Benign, LG, and HG. DRS and histopathology data were processed using MATLAB R2014a software. Background noise was subtracted from the DRS signal and the signal-to-noise (S/N) ratio was calculated. Spectral data with S/N $\leq$ 6 were excluded. Each spectrum was normalized to the area under the curve. This eliminated inter- and intra-patient variations.

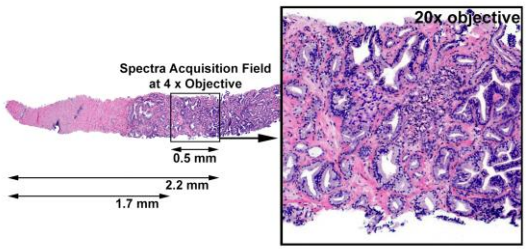

Figure 3: *Measurement window* on H&E stained biopsy core

Partial least square analysis of tissue spectra was carried out to reduce data dimension and to identify principal components (PC) that could be used as potential classifiers for tissue classification. The Wilcoxon rank-sum test was used to identify statistically significant PCs and the Pearson correlation coefficient was used to determine whether any of the statistically significant PCs were correlated or not. Statistically significant ($p < 0.05$) and least correlated PCs ($R < 0.4$) were used for tissue classification. Selected PCs were tested for their ability to differentiate between HG vs benign, HG vs LG, LG vs benign, and malignant vs benign, using support vector machine (SVM) with linear and non-linear (radial basis function) kernels. The leave-one-out cross validation method and SVM learning were employed to determine sensitivity, specificity, negative predictive value, and positive predictive value for tissue classification between each diagnostic category.

III. EXPERIMENTS AND RESULTS

Twenty patients consented to this study. A total of 187 viable biopsy cores were included in the analyses. By histopathology, 29 were classified as HG cancer, 49 as LG cancer, and 109 as benign. *Fig. 4* shows the mean DRS for each diagnostic category. There are clearly visible differences in the mean spectra between the diagnostic categories largely between 500-650 nm. Notable features are relative changes of intensities, absorptions at specific wavelengths, and slope variations. These features may be attributed to the altered architecture of the malignant glands as shown in *Fig. 1*. Thus, DRS may contain information regarding morphological features of different Gleason grades, including spacing between glands, infiltration rate, fusion of glands, and loss of glandular architecture.

Table I summarizes the performance parameters for tissue classification using SVM with linear kernel function. These results show that the optical biopsy needle based on DRS can potentially differentiate HG cancer from LG cancer and benign tissue with high degree of accuracy. DRS failed to diagnose (false negatives) 6-10 out of 29 HG cancers (21-35%) depending on the combination of PCs used and classification type. DRS provide sufficient accuracy for differentiating malignant lesions from benign tissue to increase the diagnostic yield of TRUS biopsies while reducing high false negative rates [13]. SVM with non-linear kernel functions gave similar results.

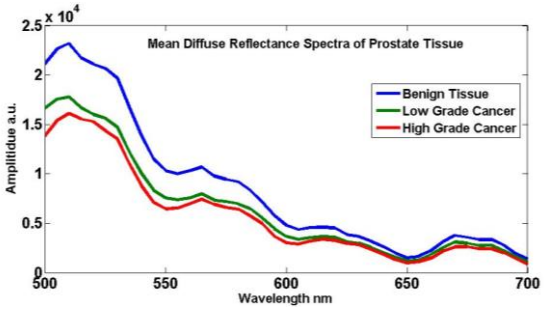

Figure 4: Mean diffuse reflectance spectra of benign tissue (blue), low grade cancer (green), and high grade cancer (red)

TABLE I. PERFORMANCE OF THE TISSUE CLASSIFICATION ALGORITHM

Classification Type and Selected Principal Components	Sensitivity	Specificity	Negative Predictive Value	Positive Predictive Value	False Negative HG Cancers	False Negative LG Cancer
High Grade vs Benign						
PC#: 1,2,6	66%	91%	91%	66%	10	-
PC#: 1,2,4,6	72%	83%	92%	53%	8	-
PC#: 1,3,4,6	**76%**	**80%**	**93%**	**50%**	**7**	-
High Grade vs Low Grade						
PC#: 1,3,5	66%	71%	78%	58%	10	14
PC#: 1,5	79%	67%	85%	59%	6	16
PC#: 1,2,5	69%	73%	80%	61%	9	13
PC#: 1,5,6	**76%**	**73%**	**84%**	**63%**	**7**	13
Low Grade vs Benign						
PC#: 1,2,3	61%	77%	82%	55%	-	19
PC#: 1,2,5	63%	72%	81%	51%	-	18
PC#: 1,2,7	63%	75%	82%	53%	-	18
PC#: 1,2,5,7	65%	71%	82%	50%	-	17
Malignant vs Benign						
PC#: 1,2,3,5	69%	73%	77%	65%	7	17
PC#: 1,2,3,7	**68%**	**76%**	**77%**	**67%**	**7**	18

In a previous study, we analyzed auto fluorescence spectra (AFS) collected using this needle for the same biopsy cores. Study results showed 86% sensitivity, 87% specificity, 90% negative predictive value, and 83% positive predictive value for malignant versus benign prostate tissue classification using 290, 330, 340, and 350 nm excitations [14]. AFS also failed to diagnose (false negatives) 0-7 HG cancer (0-24%) depending on the excitation wavelengths and combination of PCs used. Hence, use of either DRS or AFS or both may potentially improve diagnostic accuracy of TRUS biopsies by precise targeting of HG prostate cancer.

IV. Conclusion

We have demonstrated the potential of DRS to accurately differentiate HG prostate cancer from LG cancer and from benign tissue. Hence, a TRUS-guided optical biopsy needle can be used for more precise targeting of HG prostate cancer lesions for assessment of the *correct GS* of the disease and reduce high false negative rates of initial TRUS biopsies. Additional studies are required to confirm these findings.

REFERENCES

[1] R. L. Siegel, K. D. Miller, and A. Jemal, "Cancer statistics, 2016," *CA Cancer J. Clin.*, vol. 66, no. 1, pp. 7-30, Jan.2016

[2] H. B. Carter, P. C. Albertsen, M. J. Barry, R. Etzioni, S. J. Freedland, K. L. Greene, L. Holmberg, P. Kantoff, B. R. Konety, M. H. Murad, D. F. Penson, and A. L. Zietman, "Early Detection of Prostate Cancer: AUA Guideline," *J. Urol.*, May2013

[3] D. F. Gleason and G. T. Mellinger, "Prediction of prognosis for prostatic adenocarcinoma by combined histological grading and clinical staging," *J Urol.*, vol. 111, no. 1, pp. 58-64, Jan.1974

[4] J. I. Epstein, "An update of the Gleason grading system," *J. Urol.*, vol. 183, no. 2, pp. 433-440, Feb.2010

[5] H. Lepor and N. M. Donin, "Gleason 6 prostate cancer: serious malignancy or toothless lion?," *Oncology (Williston. Park)*, vol. 28, no. 1, pp. 16-22, Jan.2014

[6] P. M. Pierorazio, P. C. Walsh, A. W. Partin, and J. I. Epstein, "Prognostic Gleason grade grouping: data based on the modified Gleason scoring system," *BJU. Int.*, vol. 111, no. 5, pp. 753-760, May2013

[7] S. Sfoungaristos and P. Perimenis, "Clinical and pathological variables that predict changes in tumour grade after radical prostatectomy in patients with prostate cancer," *Can. Urol. Assoc. J.*, vol. 7, no. 1-2, p. E93-E97, Jan.2013

[8] F. K. Chun, T. Steuber, A. Erbersdobler, E. Currlin, J. Walz, T. Schlomm, A. Haese, H. Heinzer, M. McCormack, H. Huland, M. Graefen, and P. I. Karakiewicz, "Development and internal validation of a nomogram predicting the probability of prostate cancer Gleason sum upgrading between biopsy and radical prostatectomy pathology," *Eur. Urol.*, vol. 49, no. 5, pp. 820-826, May2006

[9] R. Richards-Kortum and E. Sevick-Muraca, "Quantitative optical spectroscopy for tissue diagnosis," *Annu. Rev. Phys. Chem.*, vol. 47, pp. 555-606, 1996

[10] O. M. A'amar, L. Liou, E. Rodriguez-Diaz, M. A. De Las, and I. J. Bigio, "Comparison of elastic scattering spectroscopy with histology in ex vivo prostate glands: potential application for optically guided biopsy and directed treatment," *Lasers Med. Sci.*, Dec.2012

[11] V. Sharma, E. O. Olweny, P. Kapur, J. A. Cadeddu, C. G. Roehrborn, and H. Liu, "Prostate cancer detection using combined auto-fluorescence and light reflectance spectroscopy: ex vivo study of human prostates," *Biomed. Opt. Express*, vol. 5, no. 5, pp. 1512-1529, May2014

[12] P. N. Werahera, J. W. Daily, M. S. Lucia, A. van Bokhoven, E. D. Crawford, and F. Barnes, "Multi-Excitation Diagnostic Systems and Methods for Classification of Tissue,"US20080194969 A1, Mar.26, 2013.

[13] J. Raja, N. Ramachandran, G. Munneke, and U. Patel, "Current status of transrectal ultrasound-guided prostate biopsy in the diagnosis of prostate cancer," *Clin Radiol.*, vol. 61, no. 2, pp. 142-153, Feb.2006

[14] P. N. Werahera, E. A. Jasion, E. D. Crawford, F. G. La Rosa, M. S. Lucia, A. van Bokhoven, H. T. Sullivan, J. D. Port, P. D. Maroni, and J. W. Daily, "Systematic diagnosis of prostate cancer using an optical biopsy needle adjunct with fluorescence spectroscopy," *Conf. Proc. IEEE Eng Med Biol. Soc.*, vol. 2014, pp. 2165-2168, 2014.